

Half-integer quantization in organic superconductors

Yu. V. Nazarov

Landau Institute of Theoretical Physics, USSR Academy of Sciences

(Submitted 13 June 1988)

Zh. Eksp. Teor. Fiz. **95**, 338–347 (January 1989)

The manifestations of half-integer quantization, which is specific for definite types of superconducting pairing, are described. It is assumed that this pairing is realized in organic superconductors, and that observation of the described phenomena can confirm the validity of these assumptions. The conditions under which half-integer quantization of the magnetic flux and of the phase are directly manifested are determined. An intermediate-state vortex structure is considered and it is shown that an hexagonal lattice of half-integer vortices is realized in a wide range of magnetic fields.

INTRODUCTION

Certain distinctive properties of superconductivity in organic conductors^{1,2} can be explained by assuming a non-trivial type of superconducting pairing,³ similar to that realized in heavy-fermion compounds.^{4,5}

Favoring this assumption for the TMTSF family (Bechgaard salts) are a number of experimental facts: the strong suppression of superconductivity by impurities,⁶ possible exceeding of the paramagnetic limit for H_{c2} ,^{7,8} and non-exponential temperature dependence of NMR damping.⁹ Theoretical arguments based on the similarity of the compounds of the TMTSF and BEDT families, and also certain experimental data,¹⁰ allow us to speak, albeit with less assurance, of a nontrivial type of pairing also as applied to BEDT salts.

The possible types of pairing in heavy-fermion compounds are listed in Ref. 5. The main features distinguishing these compounds from organic conducting materials are the quasi-one (two)-dimensional character of the electron spectrum and the smallness of the spin-orbit interaction. This leads to approximate symmetries connected with conservation of the spin and of the number of carriers on each chain. A classification of the possible type of pairing with account taken of the various features is given in Ref. 11, and some data important for the understanding of the symmetry aspect of the problem are given in the Appendix.

The following types of pairing were proposed for the description of superconductivity in Bechgaard salts:

$$\hat{\Delta}(\mathbf{k}) = i\sigma_y(n_0 \cos k_b b + i n_0 \sin k_b b) \exp(i\varphi) \quad (\text{phase } A) \quad (1a)$$

in Ref. 12 and

$$\hat{\Delta}(\mathbf{k}) = i\sigma_y(\sigma \mathbf{d}) f(k_a) \exp(i\varphi), \quad -f(k_a) = f(-k_a) \quad (\text{phase } B) \quad (1b)$$

in Ref. 13. Standard designation of the axes^{1,2} is used. If the approximate symmetries mentioned are regarded as exact, the order parameter in these phases is continuously degenerate: the energy depends only on the modulus of the four-dimensional vector (n_0, \mathbf{n}) or of the three-dimensional one \mathbf{d} .

Phases *A* and *B* have a common property: the order parameter remains unchanged under the substitution $(n_0, \mathbf{n}) \rightarrow (-n_0, -\mathbf{n})$ ($\mathbf{d} \rightarrow -\mathbf{d}$) and a simultaneous shift $\varphi \rightarrow \varphi + \pi$ of the gauge phase. As shown in Refs. 14 and 15, such a property of the order parameter in He^3 -*A* makes pos-

sible the existence of vortices with half magnetic flux quanta. In a superconductor, analogously, this property causes the change of the gauge phase on tracing a closed contour to equal either $2\pi n$, as in the case of ordinary pairing, or $\pi + 2\pi n$. In the latter case a texture of the order parameter (n_0, \mathbf{n}) , \mathbf{d} exists.

The purpose of the article is an analysis of the physical manifestations of this half-integer quantization.

FREE ENERGY AND CHARACTERISTIC SCALES

Effects due to the approximate continuous degeneracy of the order parameter manifest themselves at distances much larger than the superconductivity correlation length ξ . This makes it possible to assume in the expression for the free energy that $n_0^2 + \mathbf{n}^2$ and \mathbf{d}^2 are constant, and retain only terms of second order in the gradients and terms that violate the approximate symmetry. For phase *A*, the free-energy density is

$$F_A = a_{\alpha\beta}^A \left(\nabla_\beta \varphi \nabla_\alpha \varphi + \frac{\partial n_0}{\partial x^\alpha} \frac{\partial n_0}{\partial x^\beta} + \frac{\partial \mathbf{n}}{\partial x^\alpha} \frac{\partial \mathbf{n}}{\partial x^\beta} \right) + b_{\alpha\beta}^A \nabla_\alpha \varphi \nabla_\beta \varphi + c_{\alpha\beta} + v_0 n_0^2 + \mathbf{n} \hat{\nu} \mathbf{n}. \quad (2a)$$

For phase *B* we have a similar expression:

$$F_B = a_{\alpha\beta}^B \left(\nabla_\beta \varphi \nabla_\alpha \varphi + \frac{\partial \mathbf{d}}{\partial x^\alpha} \frac{\partial \mathbf{d}}{\partial x^\beta} \right) + b_{\alpha\beta}^B \nabla_\alpha \varphi \nabla_\beta \varphi + \mathbf{d} \hat{\nu} \mathbf{d}. \quad (2b)$$

The Greek subscripts denote here the Cartesian components of the coordinates, and boldface symbols are retained for vectors in spin space.

Let us estimate the scale of the coefficients in (2a) and (2b). The quantity v_0 has a smallness connected with the strong anisotropy of the electron spectrum $v_0 \sim (t_b/t_a)^2 \varepsilon$, where ε is the difference between the free-energy densities in the superconducting and normal states, $t_{a,b}$ are the hop-over integrals along the axes *a* and *b* respectively, i.e., $v_0 \sim 10^{-2} \varepsilon$. The tensor $\hat{\nu}$ describes spin-orbit effects and can be estimated at¹⁶

$$\hat{\nu} \sim (e^2/\hbar c)^2 \varepsilon \sim 10^{-4} \varepsilon.$$

We see that $v_0 \gg \hat{\nu}$. In this case, depending on the sign of v_0 , the pairing in the homogeneous state of phase *A* is either singlet ($\mathbf{n} = 0$, phase *A*₁) or triplet ($n_0 = 0$, phase *A*₂). The tensor $\hat{\nu}$ lifts the degeneracy remaining in the triplet case.

The tensor $a_{\alpha\beta}$ has the usual scale of magnitude. In the BCS approximation, $c_{\alpha\beta} \equiv 0$ and $b_{\alpha\beta} \equiv 0$. It can be verified that allowance for Fermi-liquid effects leads to $b_{\alpha\beta}, c_{\alpha\beta} \lesssim a_{\alpha\beta}$ at $T \lesssim T_c$. Near T_c , $c_{\alpha\beta}$ and $b_{\alpha\beta}$ are proportional to the fourth power of the order parameter, i.e., $c_{\alpha\beta}, b_{\alpha\beta} \sim (T - T_c)^2$, whereas $a_{\alpha\beta} \sim |T - T_c|$. We assume hereafter that $a_{\alpha\beta} \gg b_{\alpha\beta}, c_{\alpha\beta}$.

The gradient terms and terms that violate the approximate symmetry in (2a) and (2b) become comparable on scales of the order of the anisotropy length $l_{an} \sim (v/a)^{1/2}$. On smaller scales the directions of the vectors (n_0, \mathbf{n}) and \mathbf{d} can differ substantially from the most favorable one in the homogeneous state. It is useful to cite numerical estimates: $l_{an} \sim 10^{-1} \xi$ for phase A_1 and $l_{an} \sim 10^{-2} \xi$ for phase A_2 and B . In strongly anisotropic organic-superconductor crystals the scale of ξ depends on the direction of the change of the order parameters, and estimates based on magnetic measurements yield $10^{-5} - 10^{-6}$ cm. The magnetic-field penetration depth is $\lambda \sim 10^{-4} - 10^{-3}$ cm, and reaches 10^{-2} cm in BEDT salts if the magnetic field is parallel to the chains. We have thus always $l_{an} \ll \xi$, while the ratio of λ and l_{an} can be arbitrary.

DIRECT OBSERVATION OF HALF-INTEGER QUANTIZATION

Let us see how magnetic flux is quantized under the conditions of classical experiments¹⁷—in a hollow cylinder with sufficiently thick walls ($l \gg \lambda$). A half-integer number of flux quanta corresponds to a change of the phase φ by $2\pi n + \pi$ after circling around the cavity. It can be seen from (1a) and (1b) that the order parameter is continuous if $(n_0, \mathbf{n}) \rightarrow (-n_0, \mathbf{n})$ for this circling or respectively $\mathbf{d} \rightarrow -\mathbf{d}$. The vector is then deflected from the energywise most favored direction, producing a texture, and this leads to loss of energy E_0 per unit cylinder length. The equilibrium value of the flux Φ_{int} contained in the cavity is determined from the condition that the Gibbs potential be a minimum:

$$G = (\Phi_{ext} - \Phi_{int})^2 / 8\pi S + E_0 m, \quad \Phi_{int} = \Phi_0 (n + m/2), \\ n = 0, \pm 1, \pm 2, \dots, \quad m = 0, 1.$$

Here S is the area of the cavity, $\Phi_0 = \hbar c / 2e$, and Φ_{ext} is the flux of the external magnetic field through the cavity. The result is shown in Fig. 1. If $E_0 < \Phi_0^2 S / 32\pi$, the flux is half-integer at certain values of the external field.

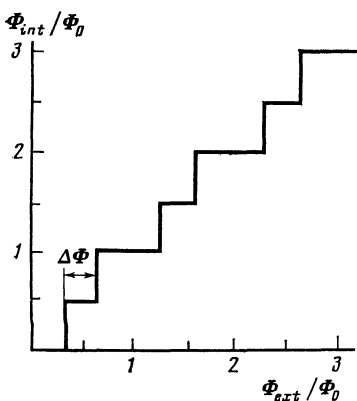


FIG. 1. Dependence of trapped magnetic flux on the external field at $E_0 < \Phi_0^2 S / 32\pi$. The experimentally determined quantity is $\Delta\Phi = \Phi_0 (1 - E_0 32\pi / \Phi_0^2 S) / 2$.

The form of the texture depends on the ratio of the cylinder radius R and the length l_{an} introduced above. If $R \gg l_{an}$, one soliton wall joining the inner and outer surfaces of the cylinder suffices to meet the quantization condition. By varying (2a) and (2b) it is easy to determine the shape and energy of such a wall. We parametrize the vectors characterizing the order parameter in the following fashion:

$$\begin{aligned} n_0 &= \cos \chi & n_1 &= \cos \chi & d_1 &= \cos \chi \\ n_2 &= \sin \chi \text{ (phase } A_1); & n_2 &= \sin \chi \text{ (phase } A_2); & d_2 &= \sin \chi \text{ (phase } B). \\ n_{2,3} &= 0 & n_{0,3} &= 0 & d_3 &= 0 \end{aligned} \quad (3)$$

We obtain for χ the sine-Gordon equation

$$\chi = 2 \operatorname{arctg} \exp 2x/l_{an}, \quad E_0 = 2ll_{an} a_{xx}, \\ l_{an}^{-1} = [(v_{11} - v_{22}) a_{xx}]^{1/2},$$

where l is the cylinder-wall thickness. This yields the condition for observing half-integer quantization:

$$lS \leq (\pi\lambda)^2 l_{an} / 2 \leq 10^{-8} \text{ cm}^3. \quad (4)$$

Since the cylinder is made of an anisotropic material, the values of λ and l_{an} are not constant on circling around the cavity. It is necessary to substitute in (4) the maximum value of λ and the minimum value of l_{an} . For $l_{an} \gg \lambda$ the condition (4) is compatible with the condition for sufficient wall thickness and specifies micron scales for l and S . It must be noted that the soliton wall described above is a topologically nontrivial object, so that a state with half-integer number of flux quanta is metastable and can in principle be observed also if the condition (4) is not met.

It is probably simpler to observe effects of half-integer phase quantization, i.e., phenomena in SQUIDS. Such effects in Josephson chains containing superconductors with normal and nontrivial pairing have been considered in Ref. 18. Here we shall describe the behavior of a SQUID made up entirely of an organic conductor. The SQUID consists of two bridges joining the banks and limiting the aperture the magnetic flux Φ through which is specified (Fig. 2). The change

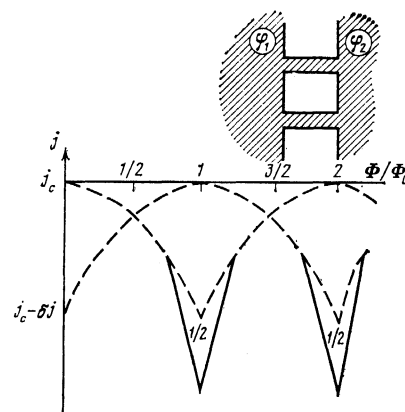


FIG. 2. Two-contact SQUID in an external magnetic field. The dashed curves show the dependences of the critical current on the external field in the integer and half-integer SQUID states. The solid lines are the boundaries of the field and current values at which the half-integer SQUID state is energywise favored.

of the gauge phase φ on circling around the aperture over the bridges, just as in the example considered above, is a multiple of 2π if there is no texture and is equal to $2\pi n + \pi$ if the corresponding texture is present. It is known that the critical current of a SQUID varies periodically as a function of Φ . We consider below a case when the maximum change of current is $\delta j \ll j_c$. The free energy of the bridge as a function of the phase difference between the banks can be expanded about the value of φ_0 at which the current is a maximum:

$$F(\varphi) = F_0 + (\hbar/e) [j_0(\varphi - \varphi_0) - \delta j(\varphi - \varphi_0)^3/3\pi^2], \quad (5)$$

$$j(\varphi) = j_c - \delta j(\varphi - \varphi_0)^2/3\pi^2.$$

By virtue of the approximate symmetry, the force $F(\varphi)$ is almost independent of the presence of a texture.

If the current is lower than critical, the SQUID can be in two states, one of which is metastable: integer, in which case

$$\varphi_1 - \varphi_2 + 2\pi\Phi/\Phi_0 = 2\pi n$$

and half-integer, in which case

$$\varphi_1 - \varphi_2 + 2\pi\Phi/\Phi_0 = 2\pi n + \pi. \quad (6)$$

We assume the bridges to be equal. The critical currents in the integer and half-integer states are

$$j = 2(j_c - \delta j\alpha^2), \quad j = 2[j_c - \delta j(\alpha - 1)^2/\pi^2],$$

where $\alpha = \arccos \cos(\Phi/\Phi_0)$. From (5) and (6) we find that at certain values of the current and magnetic flux the half-integer state can be energywise favored if the texture energy is $E_0 < \hbar j_c \pi / e 2^{1/2}$. These values are determined from the inequality ($\gamma = eE_0 2^{1/2} / \pi \hbar j_c$)

$$\gamma < (\alpha - 1/2)^{1/2}, \quad (7)$$

$$j < \delta j \{ \alpha^2 + [(2\alpha - 1)/\gamma - \gamma]^2 / 4 \}$$

(see Fig. 2). If the bridge is much longer than l_{an} the texture is a soliton wall located inside the bridge. In the inverse case the texture is localized on the banks near one of the bridges. The energy texture is described in this case by the equation $E_0 \sim \alpha l'$, where l' is the characteristic dimension of the bridge cross section. Relations (7) make it possible to determine this energy from the experimental data.

VORTEX LATTICES

The materials considered are type-II superconductors with high values of κ . Interest attaches therefore to a mixed-state vortex structure. In principle one might expect the appearance of half-integer vortices similar to those described in Ref. 15 for $\text{He}^3\text{-A}$. The energy of an isolated half-integer vortex, however, is infinite and such objects can appear only in pairs (confinement) bound by a soliton wall, at distances much larger than l_{an} . The vortices attract thus each other at large distances. The short-distance-interaction sign, which determines whether it is convenient for the vortices to coalesce or to form a molecule of finite size, turns out to depend on the parameters that enter in Eqs. (2a) and (2b).

Let us consider an isolated pair of half-integer vortices in greater detail. We transform expressions (2) for the free energy. The strong anisotropy of the material greatly com-

plicates the problem, but seems to affect the qualitative results little. We introduce therefore the following simplifying assumptions: $b_{\alpha\beta} = \beta a_{\alpha\beta}$, $1/\kappa \ll \beta \ll 1$, with $c_{\alpha\beta} = 0$ (recall that the latter is certainly valid if $1 \gtrsim |T - T_c|/T_c \gtrsim 1/\kappa$), the magnetic field is directed along one of the principal axes of the symmetric tensor $a_{\alpha\beta}$; since the material is monoclinic, these axes are different from, albeit close to, the directions of the smallest periods of the crystal. The problem becomes in this case planar and an affine transformation of the coordinates and of the vector-potential changes the equations to a form that is isotropic in this plane.¹⁰ We parametrize the vectors (n_0, \mathbf{n}) and \mathbf{d} in accordance with (3). The free energy takes then the form

$$\mathcal{F} = \int dx dy \left[\left(\nabla\varphi - \frac{2e}{c} A \right)^2 + (\nabla\chi)^2 \right] \frac{a}{2}$$

$$+ \beta \frac{a}{2} (\nabla\chi)^2 + \frac{(\text{rot} A)^2}{8\pi} + \nu \sin^2 \chi$$

and in dimensionless variables

$$\mathbf{x} \rightarrow \mathbf{x}/\lambda, \quad \mathbf{A} \rightarrow \mathbf{A}/2\pi\Phi_0\lambda, \quad (8)$$

$$\mathcal{F} = \int dx dy \{ (\nabla\varphi - \mathbf{A})^2 + (\nabla\chi)^2 + \beta (\nabla\chi)^2 + (\text{rot} A)^2$$

$$+ (\lambda/l_{an})^2 \sin^2 \chi \} \Phi_0^2 (32\pi^3\lambda)^{-1}.$$

On going around the axis of a half-integer vortex, the phase φ is changed by π , and the phase χ by $\sigma\pi$, where the charge σ takes on the values ± 1 . At distances r much shorter than l_{an} and λ from the vortex axis we have $\nabla\varphi = (2r)^{-1}$, $\nabla\chi = \sigma(2r)^{-1}$. Substituting this in (8), we compare the energy of a pair of half-integer vortices separated by a distance $r_0 \ll l_{an}$, with the energy of one integer vortex. In logarithmic approximation we have

$$\Delta\mathcal{F}_{1/2+1/2-1} = -\Phi_0^2 (32\pi^2\lambda^2)^{-1} \beta \ln(r_0/\xi).$$

Thus, if $\beta > 0$ the vortices are repelled at short distances and if $\beta < 0$ they tend to come closer to a distance $\sim \xi$. Whether they coalesce ultimately or whether a vortex molecule is produced at distances of order ξ is a question that calls for a detailed analysis outside the framework of the employed gradient approximation. It must be noted, however, that this question is of little interest for an isolated pair of vortices, since it is not clear how this can be detected in experiment.

We consider hereafter the case $\beta > 0$, being interested in the structure of vortex lattices. The dimension x_0 of an isolated vortex molecule is determined from the condition that (8) be a minimum; in dimensional units we have

$$x_0 = 2\lambda\beta/(-\ln \beta)^{1/2} \quad \text{if} \quad \lambda \ll l_{an},$$

$$x_0 = 4l_{an}\beta/(-2 \ln \beta)^{1/2} \quad \text{if} \quad \lambda \gg l_{an}.$$

Evidently $x_0 \ll \lambda$ in any case and therefore, for example if visualized by the powder method, an isolated vortex molecule looks like an ordinary integer vortex.

We consider now a mixed-state structure. So long as the distance between the vortex molecules, which is set by the magnetic induction \mathbf{B} , is much larger than x_0 , the vortices form a standard rectangular lattice. By increasing the external magnetic field it is possible to decrease the period of the structure to values of order β . In this case the lattice is restructured and tends to become more symmetric (Fig. 3). A second-order phase transition produces a hexagonal lattice

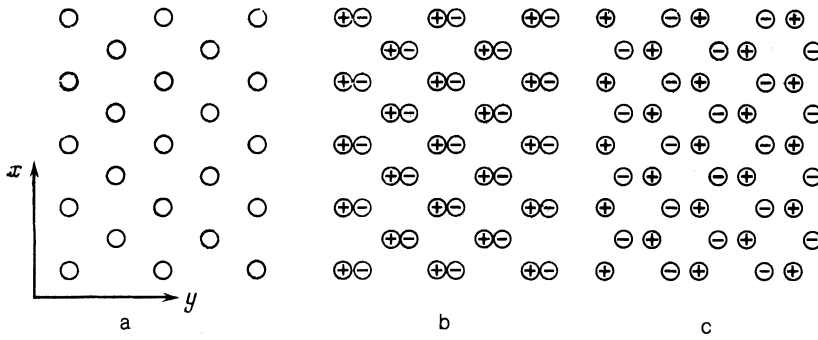


FIG. 3. Possible vortex lattices. The scales along the x and y axes differ greatly (a consequence of the anisotropy of the material): a) Triangular lattice of ordinary vortices. b) Triangular lattice of half-integer vortices; it consists of two simple sublattices that differ in the sign of the rotation of the phase χ . c) Hexagonal lattice of half-integer vortices. Separation of the sublattice by two-thirds of a period produces a structure that is more symmetric than b).

of half-integer vortices. Let us determine the critical value of the magnetic induction at which this transition takes place.

We consider first the case $\lambda \ll l_{an}$. We can neglect here the last term of (8), which is not quadratic in χ . The equations for φ and χ are then linear, and the usual method of calculating a vortex structure can be used.²⁰ We express the free energy in terms of the coordinates of the vortex axes:

$$\mathcal{F} = \sum_{h \neq 0} \pi \Phi_0^2 (8\lambda^2)^{-1} [S(\mathbf{k}) S^*(\mathbf{k}) / (1+k^2) + \mathcal{S}(\mathbf{k}) \mathcal{S}^*(\mathbf{k}) \beta / k^2] + B^2 / 8\pi, \quad (9)$$

$$S(\mathbf{k}) = \sum_i \exp(ikx_i), \quad \mathcal{S}(\mathbf{k}) = \sum_i \sigma_i \exp(ikx_i).$$

We shall need the energy difference between a triangular lattice made up of integer vortices and the lattice shown in Fig. 3a,

$$\Delta \mathcal{F} = \pi \Phi_0^2 (4\lambda^2 S_{\pi 1} S_{\text{cell}})^{-1} \sum_{b_n} (b_n^{-4} - \beta b_n^{-2}) \sin^2 b_n \zeta. \quad (10)$$

Here ζ is the separation between lattices of half-integer vortices with different charges σ , and b_n are the vectors of the reciprocal of a simple triangular lattice. It is recognized that $B \gg H_{c1}$ because $\beta \ll 1$, and the leading terms in $1/B$ are retained. This expression has at $\zeta = 2\pi/3B^{1/2}$ an extremum (a minimum for $B > B_c$) corresponding to an hexagonal lattice. By expanding $\Delta \mathcal{F}$ in terms of ζ near the extremum we determine B_c . In dimensional units we have

$$B_c = 0,092 \Phi_0 \lambda^2 / \beta.$$

In the limit $l_{an} \ll \lambda$ we can use the fact that $B_c \gg 1$ and $B_c \gg (\lambda / l_{an})^2$, and take the terms of (8) proportional to β and $(\lambda / l_{an})^2$ into account by perturbation theory. The sublattice separation is determined from the minimization condition

$$\delta \mathcal{F} = (\lambda / l_{an})^2 \int dx dy \sin^2 \chi - \beta \int (\nabla \chi)^2 dx dy.$$

It is necessary here to choose for χ the zeroth perturbation-theory approximation,

$$\chi = \text{Im} \sum_i \sigma_i \ln(z - z_i), \quad z = x + iy,$$

where x_i and y_i are the vortex coordinates. The critical induction is determined from the condition $\partial^2(\delta \mathcal{F}) / \partial \zeta^2$

($\zeta = 2\pi/3B^{1/2}$) and is equal to (in dimensional units)

$$B_c = 0,36 \Phi_0 I_{an}^2 / \beta.$$

Vortex lattices are investigated in diffraction experiments. The arrangement of the reflections is shown in Fig. 4. For $B \lesssim H_{c1}$ the relative intensity of the reflections is the same as for a simple triangular lattice. With increase of field, the intensities of the crossed reflections of the figure decrease, and at $B = B_c$ they are completely extinguished. It would be of interest to observe such a pattern via small-angle neutron diffraction. Unfortunately, estimates of the magnetic-field modulation that determines the neutron coherent-scattering cross section yield values of order 0.1–10 G, smaller by two orders of magnitude than those detected in experiments.²¹ It is possible that magneto-optic methods of investigating the vortex structure²¹ would be more suitable in this case.

MIXED STATE NEAR H_{c2}

It was shown above that in fields $B_c < B < \tilde{H}_{c2}$ the most favored is an hexagonal lattice of half-integer vortices. In fields $B \lesssim H_{c2}$, when the vortex cores overlap, the foregoing analysis is not applicable. We consider below the mixed-

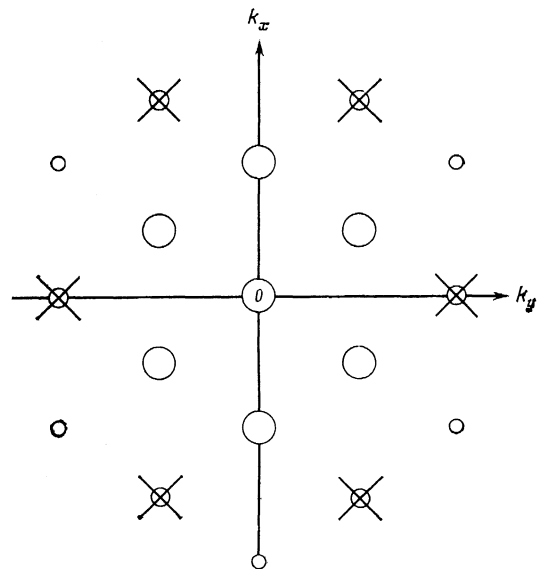


FIG. 4. Diffraction pattern of the lattices shown in Fig. 3. With increase of the separation between the sublattices the intensities of the crossed reflections decrease and d vanishes for an hexagonal structure.

state structure H_{c2} and T_c for phase B . The Ginzburg–Landau free energy is given by²²

$$\mathcal{F} = \int d^3x \left\{ \alpha \mathbf{d} \cdot \nabla + \gamma_{\alpha\beta} \left(\nabla_\alpha + \frac{2ie}{c} A_\alpha \right) d_j \left(\nabla_\beta - \frac{2ie}{c} A_\beta \right) d_j + \beta_1 (\mathbf{d} \cdot \mathbf{d})^2 - \beta_2 (\mathbf{d} \cdot \mathbf{d}') (\mathbf{d} \mathbf{d}') + f_{ij} d_i d_j + \frac{\hbar^2}{8\pi} \right\}.$$

We shall neglect terms describing the spin–orbit interaction. This is valid outside a narrow vicinity of the critical temperature ($|T - T_c|/T_c \ll 10^{-4}$). In the absence of a magnetic field the phase B is favored at $\beta_2 > 0$ and the non-unitary phase described in Ref. 2 is favored at $\beta_2 < 0$. Near H_{c2} , the solution of the Ginzburg–Landau equations is sought as usual in the form of a linear combination of solutions of a linearized equation with zero eigenvalue. By choosing different coefficients in these linear combinations one can construct various vortex structures. It can be shown that the energywise most favored structure corresponds to a minimum of the expansion

$$H = \beta_1 \Pi_1 - \beta_2 \Pi_2,$$

where

$$\Pi_1 = \frac{\langle (\mathbf{d} \cdot \mathbf{d}')^2 \rangle}{\langle (\mathbf{d} \cdot \mathbf{d}') \rangle^2}, \quad \Pi_2 = \frac{\langle (\mathbf{d} \cdot \mathbf{d}') (\mathbf{d} \mathbf{d}') \rangle}{\langle (\mathbf{d} \cdot \mathbf{d}') \rangle^2}, \quad \langle \dots \rangle = \frac{\int dV \dots}{V}.$$

We use here the fact that $\kappa \gg 1$. The coefficient π_1 characterizes the difference between $d(x)$ and a constant—the “packing.” The ratio π_1/π_2 shows the extent to which different components of the vector d are in phase. By way of trials we choose structures that are continuously deformable but retain the periodicity of a simple triangular lattice. We seek $d(x)$ in the form

$$\mathbf{d}(x, y) = \sum_n [(\mathbf{d}_1 + i\mathbf{d}_2) e^{-i\kappa n} + (\mathbf{d}_1 - i\mathbf{d}_2) e^{i\kappa n}] C_n \psi_n, \quad (11)$$

$$\mathbf{d}_1^2 = \mathbf{d}_2^2, \quad \mathbf{d}_1 \mathbf{d}_2 = 0, \quad C_n = 1, \quad n - \text{even}; \quad C_n = i, \quad n - \text{odd}, \\ \psi_n = \exp(2inqy) \exp[-1/2(x - 2nq)^2], \quad q^2 = \pi/3^{1/2}.$$

Here, as above, we assume the magnetic field to be described along one of the principal axes of the tensor $a_{\alpha\beta}$, and the values of x and y are obtained from the spatial coordinates by using an isotropy-inducing transformation. By investigating the positions of the zeros of (11) it is easy to see that $d(x)$ corresponds to the already considered structures shown in Fig. 3. The quantity determines the sublattice separation. For a simple triangular lattice we have²⁰

$$H = 1.16 (\beta_1 - \beta_2).$$

For the hexagonal from Fig. 3b we have

$$H = 1.04\beta_1 - 0.92\beta_2.$$

It can be seen that the change from a simple triangular to an hexagonal lattice leads to a packing gain, but since the vector component are no longer in phase, a loss is incurred in the coefficient π_2 . The structure is thus determined by the ratio β_2/β_1 . A simple triangular lattice is realized if $1/2 < \beta_2/\beta_1 < 1$, whereas for $0 < \beta_2/\beta_1 < 1/2$ the hexagonal is the most favorable. The Ginzburg–Landau expansion can be used if $\beta_2 > \beta_1$.

CONCLUSIONS

Some of the phases proposed for the description of superconductivity in organic materials have a symmetry that permits the gauge phase to change by π on going along a closed contour. These phenomena can be observed directly in traditional experiments on quantization in superconductors. Such a half-integer quantization can determine the structure of a mixed state. Observation of the described effects would identify the type of conductivity in the considered substances.

The author thanks G. E. Volovik and L. P. Gor'kov for helpful discussions of the results.

APPENDIX

We discuss here the symmetry whose spontaneous breaking yields the phase A . When a microscopic superconductivity mechanism of this type is considered, it is assumed that the electrons are repelled on one chain and attracted on neighboring chains. The Cooper pair is therefore made up of electrons located on neighboring chains

$$\Delta_{\alpha,\beta}^i \sim \langle \Psi_{\alpha,i}^+ \Psi_{\beta,i+1}^+ \rangle.$$

Here i numbers the chains, α and β are the spin indices, and Ψ^+ is the electron-creation operator. Neglecting hops between chains, the spin and the number of carriers on each chain are conserved, and the Hamiltonian of the system is invariant to the transformation

$$\Psi_{\alpha,i} \rightarrow U_{\alpha\beta}^i \Psi_{\beta,i},$$

where \hat{U}^i is an arbitrary unitary matrix. In this case $\hat{\Delta}^i$ is transformed as follows:

$$\hat{\Delta}^i = \hat{U}^i \hat{\Delta}^i \hat{U}_{i+1}^T.$$

This relation determines the space where the order parameter is degenerate for $t_b \ll \Delta$, T_c . Actually it is the inverse inequality which holds: Δ , $T_c \ll t_b \ll t_a$. It is easy to show in this case, by changing to a quasimomentum representation, that the Hamiltonian is invariant, accurate to terms of order t_a/t_b , to such transformations specified by U^i , which transform Δ that are independent of the index into Δ^i that are independent of the index i . The last condition defines a five-parameter family of transformations.

Transformations of this family leave invariant the quantities $\text{Tr} \hat{\Delta}^+ \hat{\Delta}$, $\text{Tr} \hat{\Delta}^+ \hat{\Delta} \hat{\Delta}^+ \hat{\Delta}$, and $\text{Tr} \hat{\Delta}^+ \hat{\Delta} \hat{\Delta}^T \hat{\Delta}^*$. To classify the possible phases it is convenient to change to an equivalent system of invariants:

$$\hat{\Delta} = i\sigma_y (d_0 + \mathbf{d}\hat{\sigma}), \quad 1 = d_0 d_0^* + \mathbf{d}\mathbf{d}^*, \\ I_1 = |d_0^2 - \mathbf{d}^2|^2, \quad I_2 = (\mathbf{d}\mathbf{d}^*)^2 - \mathbf{d}^2 \mathbf{d}^{\prime 2}.$$

The result is shown in Fig. 5. The vertices of the triangle correspond to phases produced from a nonsuperconducting state via a second-order phase transitions, accurate to terms of order t_b/t_a . The sides and interior of the triangle correspond to states obtained from these phases by further lowering of the symmetry. Let us describe these fundamental phases:

1. In the Efetov–Larkin phase, which is realized in the weak-binding limit,²³ $I_1 = I_2 = 0$. This phase is a mixture of a singlet and a triplet, therefore the transition to the super-

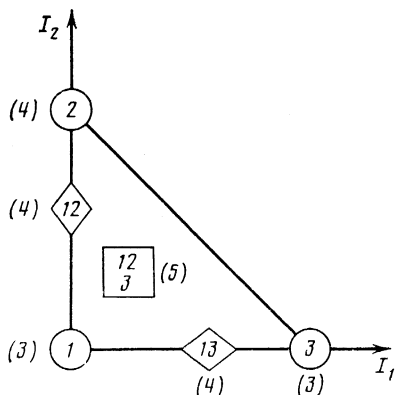


FIG. 5. Cooper pairing on neighboring chains: possible phases. The number of Goldstone modes is given in the parentheses. The following second-order phase transitions are allowed; non-superconducting state \rightarrow 1, 2, 3 \rightarrow 12, 13 \rightarrow 123.

conducting state is split when account is taken of terms of order t_b/t_1 . The heat capacity $C \sim \exp(-\Delta/T)$ as $T \rightarrow 0$.

2. In the non-unitary phase whose properties were investigated in Ref. 22, $I_1 = 0$ and $I_2 = 1$. The pairing is always triplet. As $T \rightarrow 0$ the heat capacity $iC \propto T$ and there is no superconducting gap on the entire Fermi surface.

3. The case $I_1 = 1$, $I_2 = 0$ corresponds to the phase A considered in the article. The gap has a line of zeros on the Fermi surface, and $C \propto T^2$ ($T \rightarrow 0$).

¹L. P. Gor'kov, Usp. Fiz. Nauk **144**, 381 (1984) [Sov. Phys. Usp. **27**, 809 (1984)].

²A. I. Buzdin and L. N. Bulaevskii, *ibid.* p. 413 [830].

³A. A. Abrikosov, J. Low Temp. Phys. **53**, 359 (1983).

⁴R. G. Stewart, Rev. Mod. Phys. **56**, 755 (1984).

⁵L. P. Gor'kov and G. E. Volovik, Zh. Eksp. Teor. Fiz. **88**, 1412 (1985) [Sov. Phys. JETP **52**, 843 (1985)].

⁶R. L. Greene, P. Haen, S. Z. Huang, *et al.*, Mol. Cryst. and Liquid Cryst. **79**, 539 (1982).

⁷R. Brusetti, M. Ribaut, D. Jerome, *et al.*, J. de Phys. **43**, 801 (1982).

⁸L. P. Gor'kov and D. Jerome, J. Physique Lett. **56**, 643 (1985).

⁹M. Takigawa, J. Phys. Soc. Jpn. **56**, 873 (1987).

¹⁰Y. Hasegawa and H. Fukuyama, *ibid.* p. 2619.

¹¹Y. Hasegawa and H. Fukuyama, *ibid.* **55**, 3978 (1986).

¹²Y. Hasegawa and H. Fukuyama, *ibid.* **56**, 877 (1987).

¹³L. P. Gor'kov, Pis'ma Zh. Eksp. Teor. Fiz. **44**, 537 (1986) [JETP Lett. **44**, 693 (1986)].

¹⁴G. Volovik and M. M. Salomaa, Phys. Rev. Lett. **55**, 1184 (1985).

¹⁵G. E. Volovik and M. M. Salomaa, Zh. Eksp. Teor. Fiz. **88**, 1656 (1985) [Sov. Phys. JETP **61**, 986 (1985)].

¹⁶A. V. Sokol, *ibid.* **92**, 756 (1987) [**65**, 426 (1987)].

¹⁷R. Doll and M. Nöbauer, Phys. Rev. Lett. **7**, 51 (1961). R. S. Deaver and W. M. Fairbank, *ibid.* p. 43.

¹⁸V. B. Geshkenbein, A. I. Larkin, and A. Barone, Phys. Rev. B **36**, 225 (1987).

¹⁹A. V. Balatskii, L. N. Burlachkov, and L. P. Gor'kov, Zh. Eksp. Teor. Fiz. **90**, 1478 (1986) [Sov. Phys. JETP **63**, 866 (1986)].

²⁰A. A. Abrikosov, *Fundamentals of Metal Theory* [in Russian], Nauka, 1987.

²¹R. P. Huenberg and J. P. Chen, Rev. Mod. Phys. **46**, 409 (1974).

²²L. N. Burlachkov and N. B. Kopnin, Zh. Eksp. Teor. Fiz. **92**, 1110 (1987) [Sov. Phys. JETP **65**, 630 (1987)].

²³K. B. Efetov and A. I. Larkin, *ibid.* **68**, 155 (1975) [**41**, 76 (1975)].

Translated by J. G. Adashko